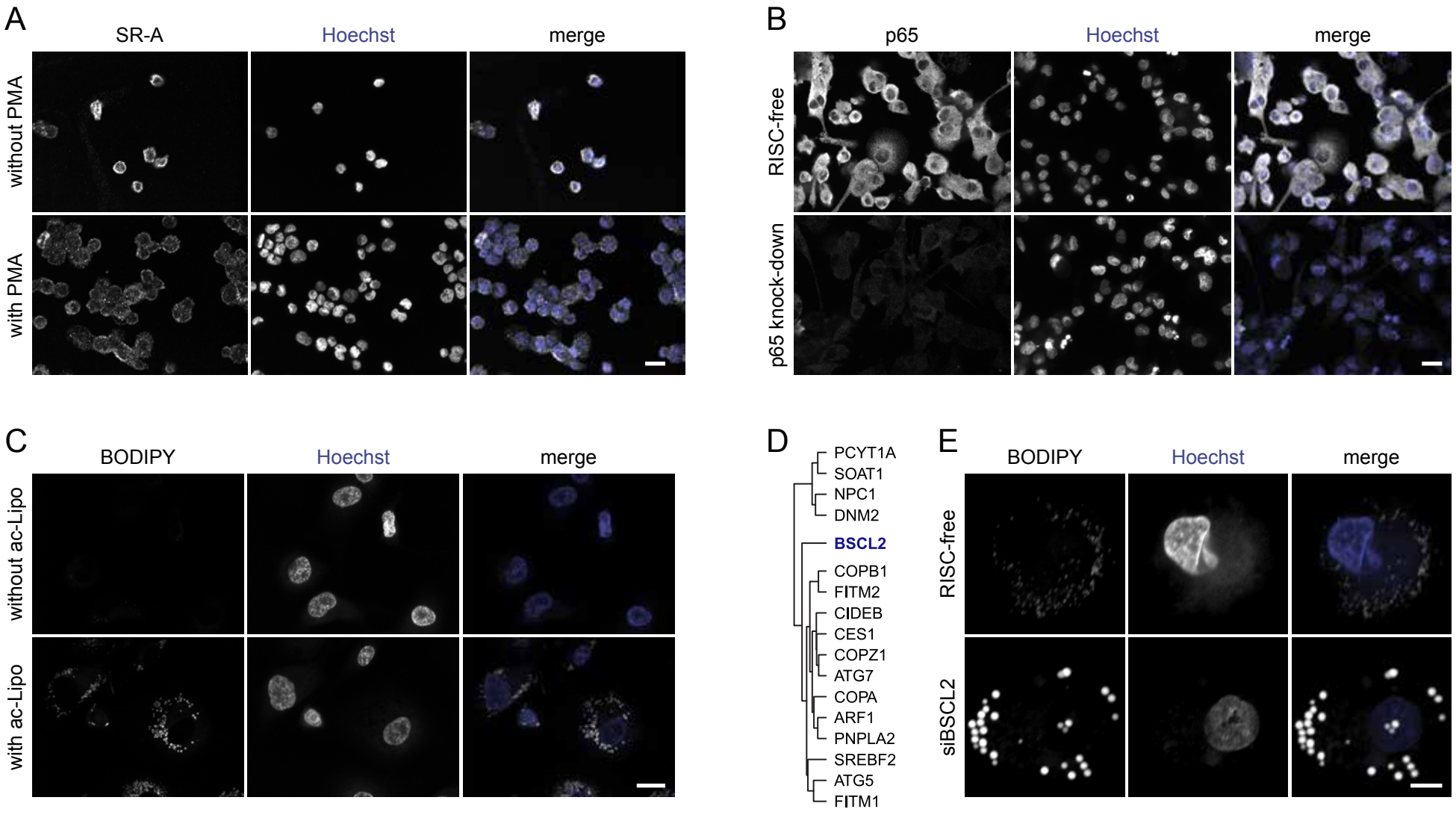

Figure S1, related to Figure 1 (Mejhert *et al.*)

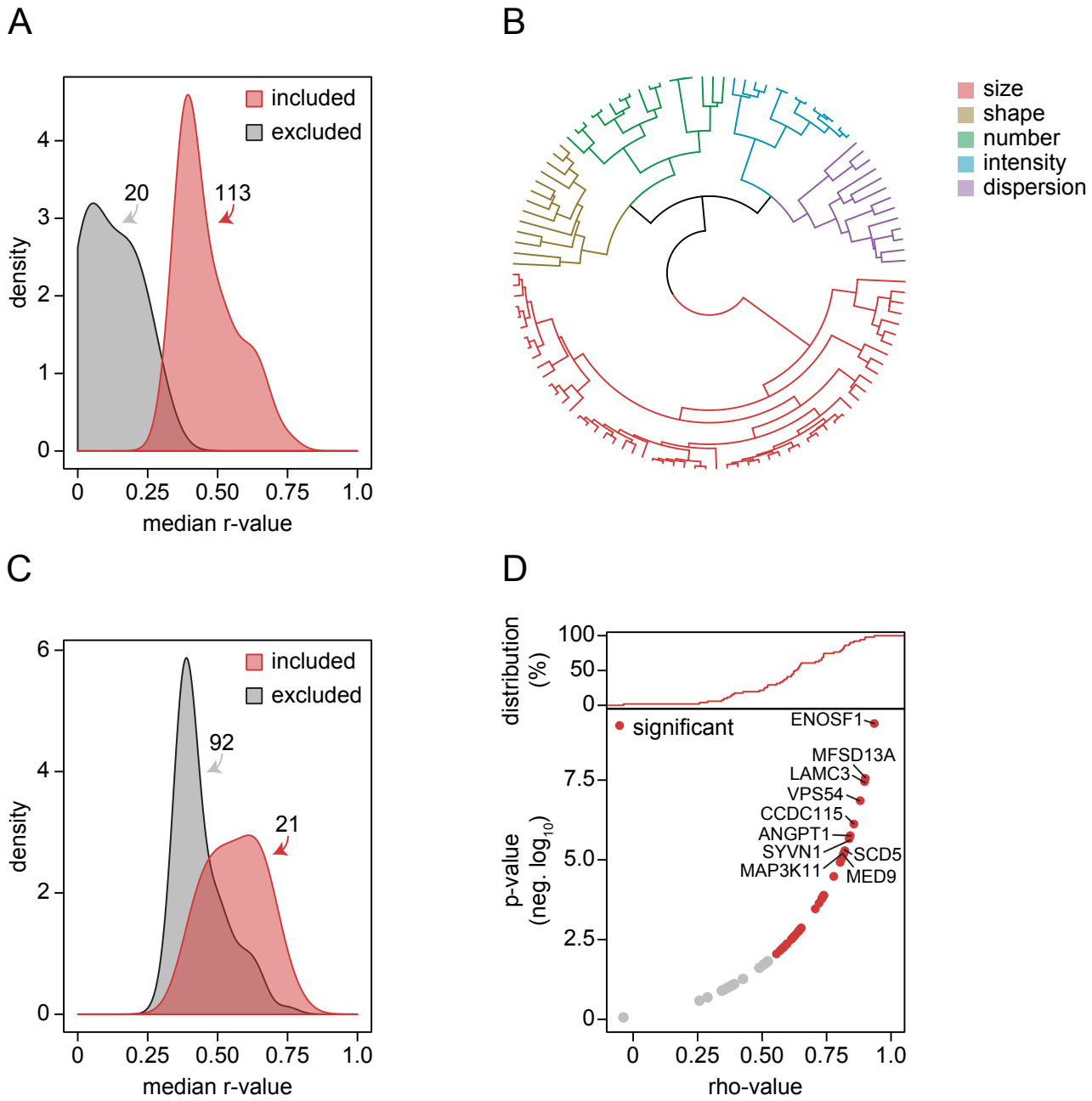

Figure S2, related to Figure 2 (Mejhert *et al.*)

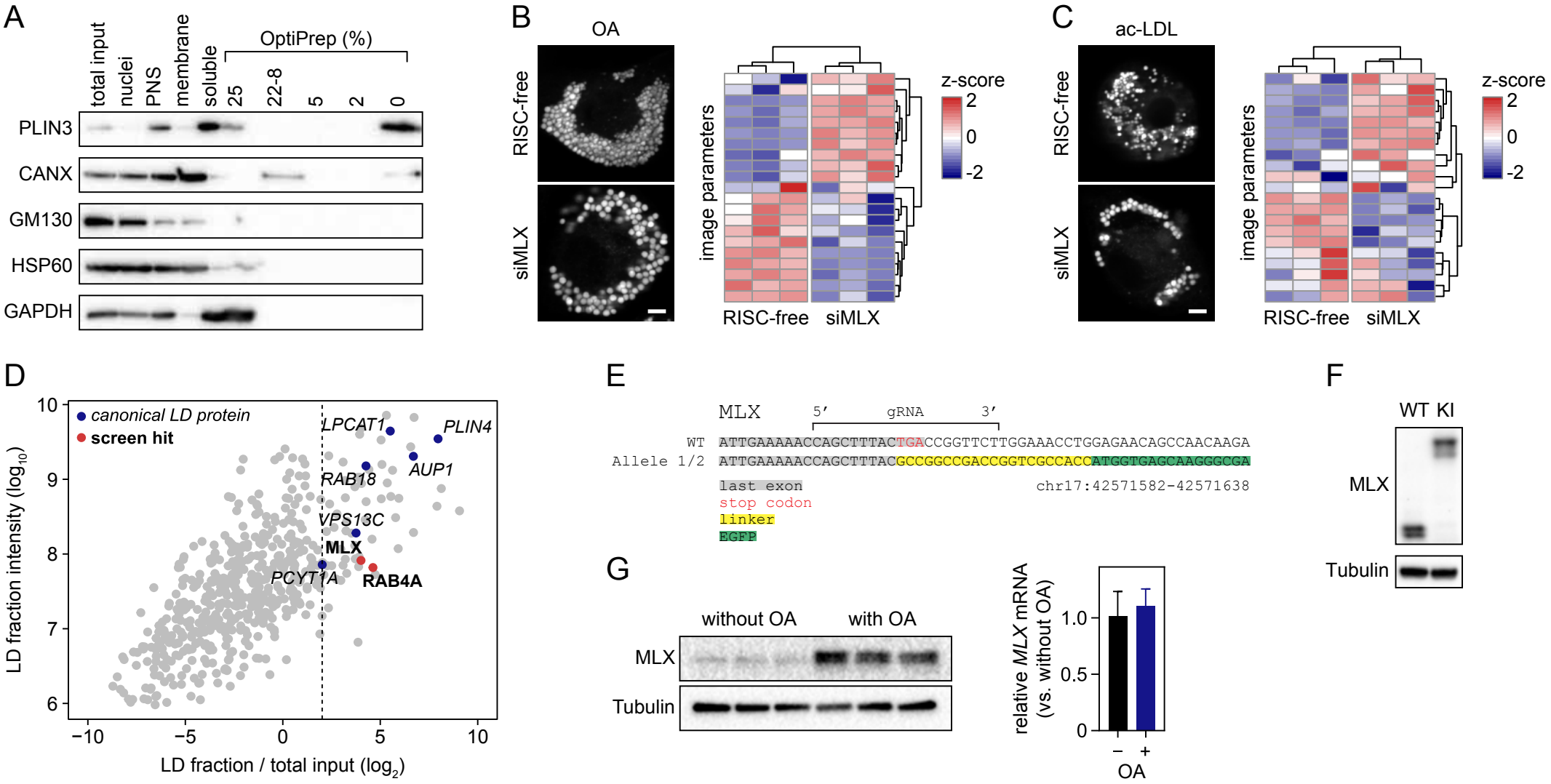

Figure S3, related to Figure 3 (Mejhert *et al.*)

Figure S4, related to Figure 4 (Mejhert *et al.*)

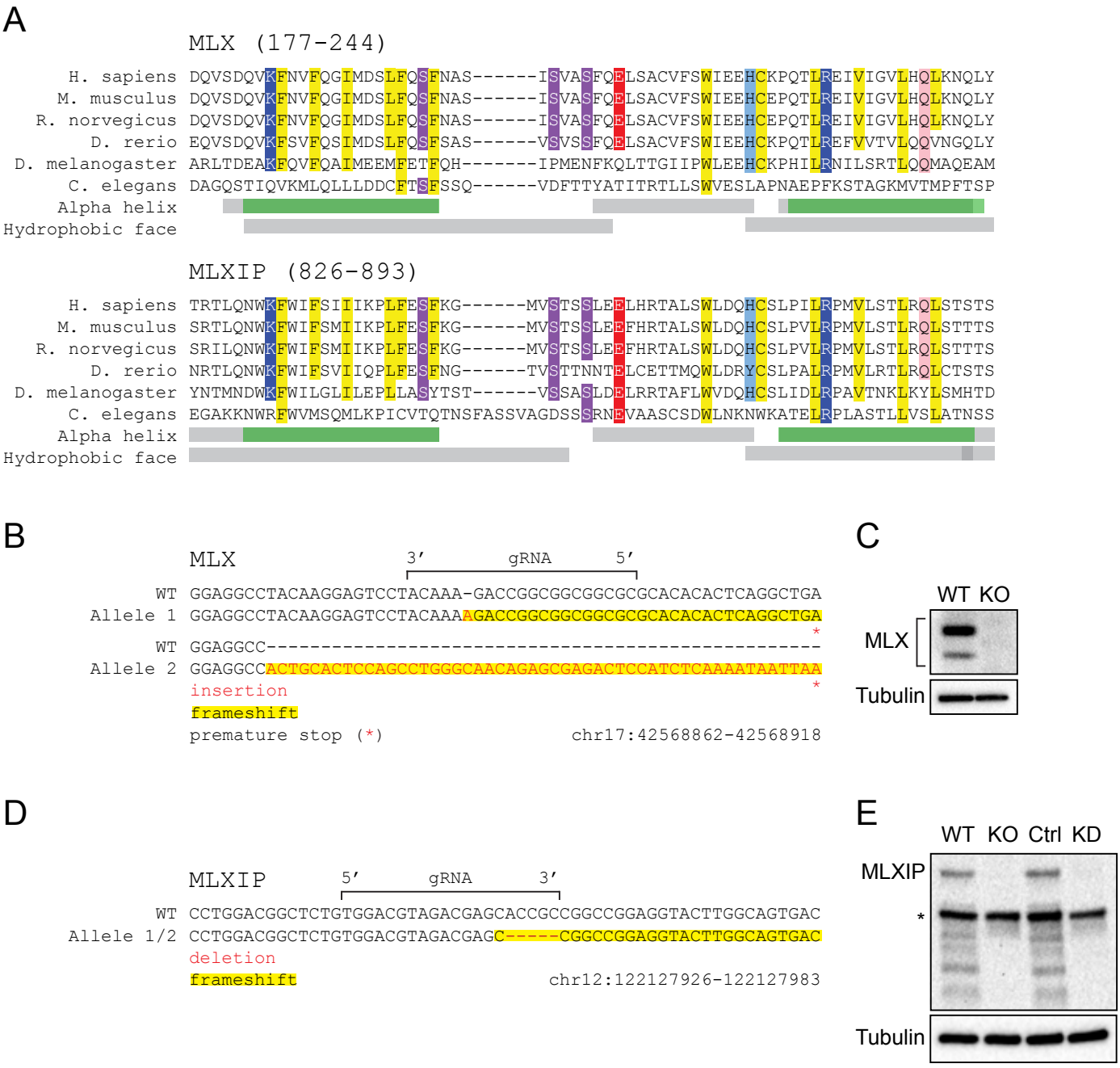

Figure S5, related to Figure 5 (Mejhert *et al.*)

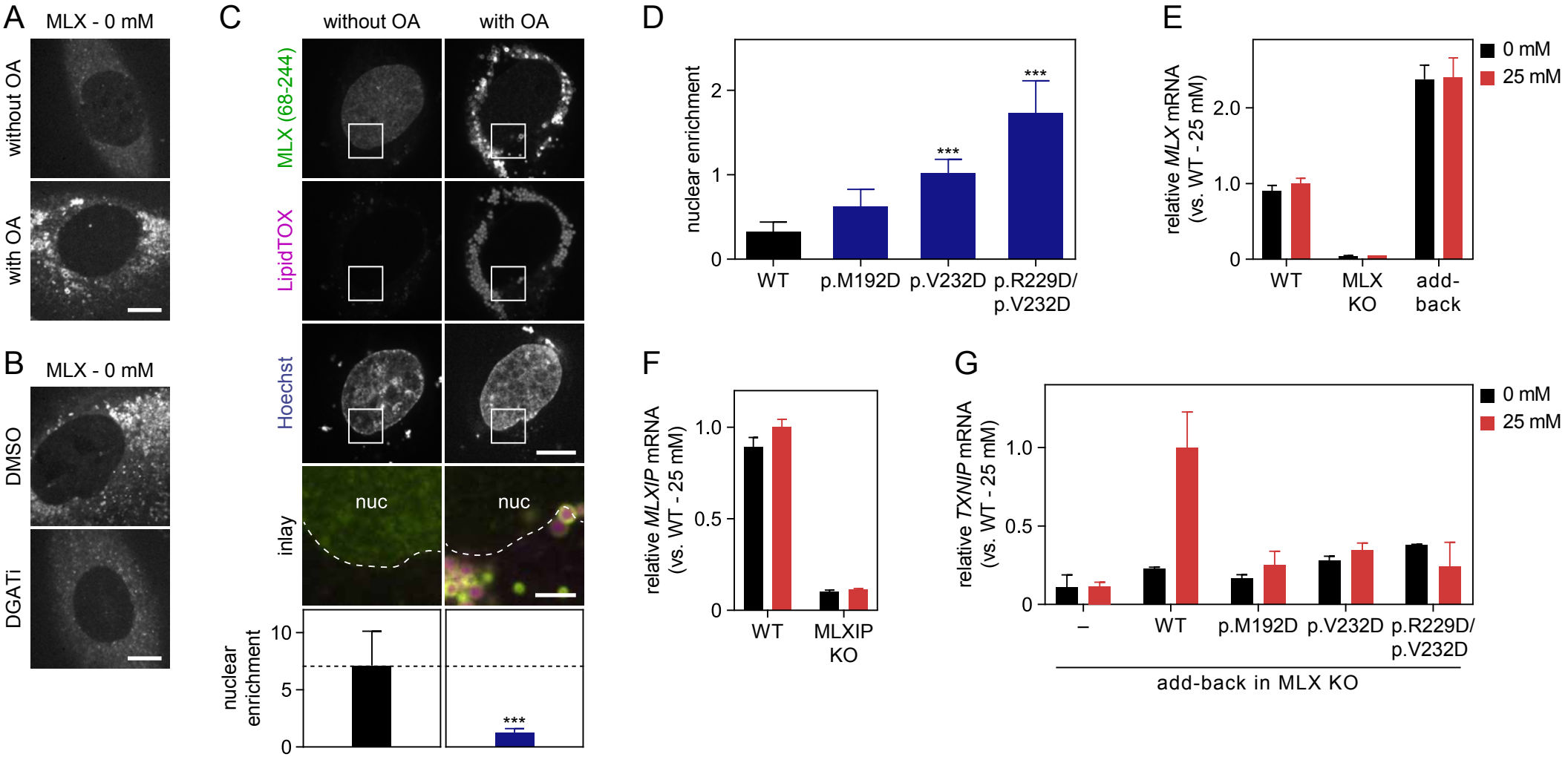

Figure S6, related to Figure 6 (Mejhert *et al.*)

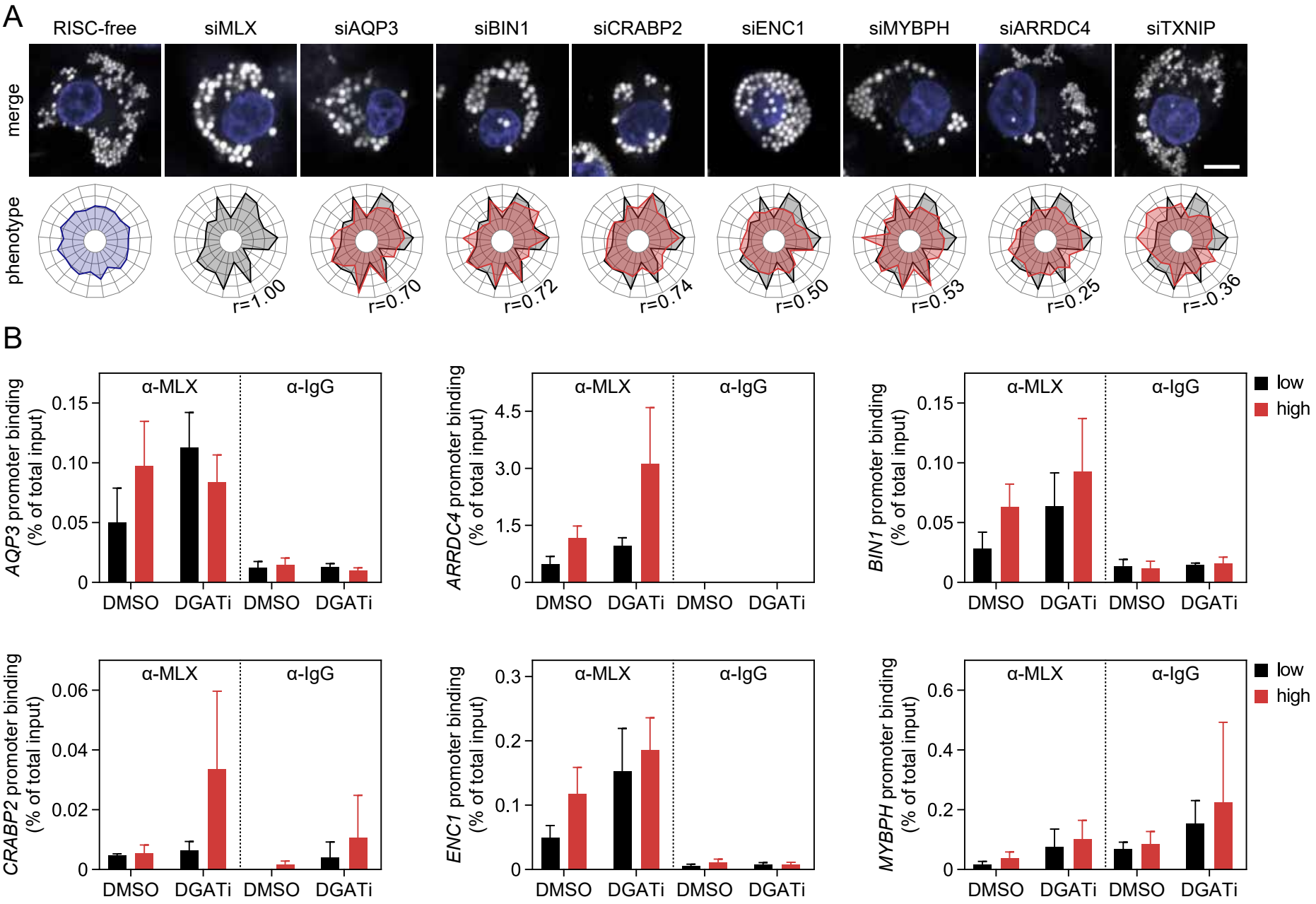

Figure S7, related to Figure 7 (Mejhert *et al.*)

SUPPLEMENTAL FIGURE TITLES AND LEGENDS

Figure S1 (related to Figure 1). Assay Optimization

(A) PMA induces differentiation of THP-1 monocytes into macrophages. THP-1 cells were seeded with or without 50 PMA for 1 day and thereafter stained for macrophage scavenger receptor 1 (SR-A) to evaluate differentiation from monocytes to macrophages. Nuclei were stained with Hoechst. Scale bar, 10 µm.

(B) THP-1 cells are efficiently transfected with siRNA. Macrophages were transfected with p65 siRNA and control RISC-free siRNA. After 3 days of knock down, the cells were stained with NFkB p65 antibody, AlexaFlour 647 secondary antibody and Hoechst. Scale bar, 10 µm.

(C) Serum starvation reduces lipid storage in macrophages. After differentiation, macrophages were washed with serum-free media and serum starved for 3 days before incubations with or without ac-Lipo. Scale bar, 10 µm.

(D-E) Pre-screening identifies known regulators of lipid storage. LDs induced by ac-Lipo addition were stained and imaged in macrophages transfected with siRNAs targeting 17 different genes. (D) Image information from six replicates per siRNA was extracted using CellProfiler and the results (median per siRNA) were evaluated using hierarchical clustering. (E) Representative confocal images of LDs (BODIPY) and nuclei (Hoechst) of macrophages transfected with either RISC-free or BSCL2 siRNAs. Scale bar, 5 µm.

For panels A-C, results from one representative experiment are shown. Abbreviations: ac-Lipo, acetylated apolipoprotein B-containing lipoprotein; PMA, Phorbol 12-myristate 13-acetate.

Figure S2 (related to Figure 2). Feature Reduction and RNAi Screen Validation

(A-C) Identification of informative image parameters. (A) The reproducibility of each image parameter was tested by pair-wise correlations comparing replicates across the genome-wide RNAi screen. Parameters with a median r-value >0.3 were included for further analyses. (B) All included image parameters were correlated against each other, and the dimensionality of the resulting correlation matrix was evaluated using hierarchical clustering. (C) Starting from the most reproducible image parameter in each major dimension, features were excluded if they covaried (|rho|>0.7) with the selected parameters and displayed low median reproducibility (r-value<0.4).

(D) Validation screening shows high reproducibility. Out of the 556 hits, 51 (~9%) were selected for re-screening using four individual siRNAs per gene. Based on the final image parameters, Spearman's rank correlation was calculated for each siRNA to compare the genome-wide RNAi screen and the validation screen. The most reproducible duplex per gene

and the cumulative distribution (%) of the duplexes are shown in the lower and upper panels, respectively. In the lower panel, significant duplexes are shown in red, and gene symbols are highlighted for the most reproducible siRNAs.

Figure S3 (related to Figure 3). LD Morphology/Composition and Regulation/Tagging of MLX

(A) Western blot confirms the separation of LDs from other organelles. THP-1 macrophages incubated in the presence of oleic acid (0.5 mM) for 6 hours were lysed and fractionated. Purity of different cellular fractions was assessed using western blotting. Results from one representative experiment are shown.

(B-C) MLX depletion alters LD morphology. Effects of MLX knockdown on LD morphology were determined in differentiated THP-1 macrophages incubated with oleic acid (0.5 mM) or ac-LDL (25 µg/mL) for 1 day. After the incubation period, cells were fixed, washed and stained with BODIPY (LDs) and Hoechst (nuclei, not shown), and images were acquired and analyzed. Left panels, confocal images of representative cells for each treatment. Scale bar, 5 µm. Right panels, clustering of the 21 extracted image parameters from three replicates of RISC-free or siMLX transfected cells.

(D) Identification of LD proteins in SUM159 cells. LD-associated proteins were determined by mass spectrometry in SUM159 cells incubated with oleic acid (0.5 mM) for 1 day. For each protein, intensities in whole-cell lysates and LD fractions were compared. Known LD proteins were used to calculate a fold-change cut-off based on the 99% confidence interval of their distribution (lower boundary is indicated by the dashed line). Results from one representative experiment are shown.

(E-F) Successful tagging of MLX in SUM159 cells. MLX was endogenously tagged with EGFP using CRISPR/Cas9-mediated engineering. Successful homologous recombination was confirmed by (E) genomic DNA PCR, followed by Sanger sequencing and (F) western blotting. For the latter, results from one representative experiment are shown.

(G) MLX protein levels are increased in cells with lipid droplets. MLX protein (left panel) and mRNA (right panel) levels were determined in SUM159 cells incubated in the absence/presence of oleic acid for 1 day. For the left panel, one representative blot is shown with three replicates per condition. For the right panel, two independent experiments, each containing three replicates, were performed. Abbreviations: ac-LDL, acetylated low-density lipoprotein; chr, chromosome; gRNA, guide RNA; KI, knock-in; OA, oleic acid; PNS, post-nuclear supernatant; WT, wild type.

Figure S4 (related to Figure 4). MLX Binds to LDs in HSL KO cells.

(A-B) Successful deletion of HSL in SUM159 cells. (A) HSL protein could not be detected by western blotting using whole cell lysates from WT and HSL KO SUM159 cells. Mouse epididymal white adipose tissue was used as a positive control. (B) CRISPR/Cas9-mediated genome editing of the *HSL* locus in SUM159 cells resulted in two alleles with frameshift mutations. For the western blot, results from one representative experiment are shown.

(C) MLX targets to LDs in HSL KO cells. WT and HSL KO cells were transfected with MLX-EGFP thereafter incubated with oleic acid (0.5 mM) for 1 day. Prior to imaging, LDs were stained with LipidTOX Deep Red. Representative images from one experiment are shown, and results were quantified (n=12 cells) using CellProfiler and evaluated using non-parametric Mann-Whitney test.

For (B-C), results are shown for HSL KO clone 3. Abbreviations: c., clone; gRNA, guide RNA; KO, knockout; WT, wild type.

Figure S5 (related to Figure 5). Alignment of MLX and MLXIP and Characterization of Knockout Cells

(A) The C-termini of MLX and MLXIP are evolutionary conserved. Multiple sequences of MLX and MLXIP derived from different species were aligned, and conserved amino acids (75% conservation threshold) identified. Secondary structures were predicted based on the human sequences. Gray boxes indicate predicted alpha helices and hydrophobic faces. Green boxes indicate putative amphipathic helix regions.

(B-E) Successful deletions of MLX and MLXIP in SUM159 cells. CRISPR/Cas9-mediated genome editing of the *MLX* locus in SUM159 cells resulted in (B) two alleles with frameshift mutations and (C) loss of MLX protein as detected by western blot. Similarly, CRISPR/Cas9-mediated genome editing of the *MLXIP* locus in SUM159 cells resulted in (D) a small deletion, which disrupted the reading frame, and (E) loss of MLXIP protein as detected by western blot. For the latter, siRNA experiments were included to support knockout results. Asterisk indicates unspecific band. For western blots, results from one representative experiment are shown. Abbreviations: chr, chromosome; ctrl, RISC-free control; KD, knockdown; KO, knockout; WT, wild type.

Figure S6 (related to Figure 6). MLX Localization/Transcriptional Activity and Characterization of Knockout Cells

(A-D) LD binding sequesters MLX away from the nuclei. Effects of alterations in lipid storage and glucose on endogenous MLX localization were determined in SUM159 cells by confocal microscopy. (A-B) Representative images of cells that were treated as described in Figure 6A-B with the exception that they were kept in 0 mM glucose media throughout the experiment. (C-D) SUM159 cells were transfected with truncated or point-mutated forms of MLX-EGFP thereafter incubated with oleic acid (0.5 mM) for 1 day. Prior to imaging, LDs and nuclei were stained with LipidTOX Deep Red and Hoechst, respectively. Representative images from one experiment are shown, and images were quantified using CellProfiler. Results were evaluated using (C) non-parametric Mann-Whitney test (n=12-14 cells) and (D) one-way non-parametric ANOVA (Kruskal-Wallis followed by Dunn's multiple comparisons test) (n=17-20 cells). Scale bars, 10 µm and 2.5 µm (inlay).

(**E-F)** *MLX* and *MLXIP* mRNAs are depleted in knockout cells. Messenger RNA levels of *MLX* and *MLXIP* were determined by qPCR in WT SUM159 cells and (E) MLX knockout clones with or without add-back of MLX by re-integration of MLX-EGFP into the *AAVS1* locus and (F) MLXIP knockout cells. The cells were starved from glucose for 2 days and thereafter incubated in the presence or absence of glucose (25 mM) for 1 day.

(G) MLX C-terminal amphipathic helices are required for transcriptional activity. WT or point-mutated versions of MLX were re-introduced in MLX KO cells by transient transfections. Cells were treated as described in panels E-F. On the second day of glucose starvation, the cells were transfected with the indicated constructs. For panels E-G, results from one representative experiment containing three replicates are shown.

Figure S7 (related to Figure 7). Lipid storage response genes regulated by MLX

(A) MLX controls a specific set of putative lipid storage response genes. For the set of genes highlighted in Figure 7A, confocal images of representative cells from the RNAi screen are displayed in the upper panel. LDs were stained by BODIPY (grey), and nuclei were stained by Hoechst (blue). Scale bar, 5 µm. In the lower panel, RNAi screen rz-scores for the 21 image parameters of each gene are visualized as radar charts. The rz-score range of the chart is set from -5 to +5 with segmentation lines at an interval of 2.5 rz-scores.

(B) MLX binding to the *ARRDC4* promoter is regulated by lipid storage. MLX occupancy of indicated target promoters in THP-1 macrophages was measured by ChIP-qPCR using IgG as a negative control. Cells were starved for glucose for 1.5 days and incubated in OA-containing media with or without glucose (10 mM) in the presence of DMSO or DGAT1/DGAT2 inhibitors for 12-16 hours. Data from three replicates are shown.